JOURNAL OF MATERIALS SCIENCE 10 (1975) 252–268

Wide angle X-ray diffraction study of the microstructure of chain-folded polyethylene crystals

A. H. WINDLE
Department of Metallurgy and Materials Science, Imperial College of Science and Technology, London, UK

The profile of the 002 diffraction peak of polyethylene is related to microstructural parameters for the [001] direction. The parameters considered are the mean crystal thickness, distribution of thicknesses, shape function and the degree of paracrystalline disorder in the lattice.

An analytical relation describing the peak profile is derived for trapezium models of the shape function. Calculations are made of peak profiles and their correlation functions for various trapezium models, levels of paracrystalline disorder and Gaussian widths for the distribution of crystal thicknesses. Particular attention is paid to the effect of these parameters on the subsidiary maxima to the 002 peak.

The 002 peak of linear polyethylene (RIGIDEX 50) crystallized from solution in xylene at 70° C is analysed in terms of the above parameters. The results are interpreted in terms of the buried fold model and indicate the presence of well defined zones of highly disordered material (probably nematic) within the crystal entities. The frequency of the zones increases as the fold surfaces are approached.

1. Introduction and scientific context

1.1. Structure of solution crystallized mats

Polymers formed by conventional techniques are never 100% crystalline. They have densities less than that calculated from the lattice unit cell, and X-ray diffraction patterns characteristic of the crystalline material are superimposed on diffuse halos which suggest the presence of an amorphous component. Electron microscopy [1] has shown polymer crystals to be thin planar entities in which the molecules fold to and fro across the thickness of the crystal, and small angle X-ray diffraction (S.A.X.D.) indicates that the planar crystals form stacks in which they are separated by thin layers of lower density material, presumed to be the amorphous component. This particular structure is known as the "two phase" model.

In terms of the two phase model, the superlattice period (long period) obtained from S.A.X.D. measurements represents the combined thickness of one crystal and one amorphous layer. It is possible, in principle, to measure the crystalline thickness from the broadening of a diffraction peak formed from lattice planes parallel to the fold surfaces, and hence obtain the amorphous thickness by subtraction from the long period. This approach has been applied to polyethylene fibres by Statton [2] and to solution crystallized polyethylene mats by Kobayashi and Keller [3] and Thielke and Billmayer [4].

This paper reports work which is the resumption of the research programme initiated by Kobayashi and Keller. These authors developed a technique of preparing well oriented mats of solution crystallized high density polyethylene. The marked texture has the result that the 002 peak is appreciably intensified when recorded using a powder diffractometer. They measured the half breadth of the 002 peak, and after correction for spectral and slit broadening obtained mean values of crystal thickness which were about 20% less than the long period – a result in accord with the two phase model.

In the current work the complete profile of the 002 peak has been subjected to close analysis using Fourier methods and the results obtained,

in addition to putting values to crystal thicknesses, have provided some further insight into the structure of the fold surfaces themselves. They also further qualify the relevance of the two phase model to solution crystallized material.

In melt crystallized polymers the amorphous layers, which are germain to the two phase model, may consist either of molecules totally separate from those in the crystals or of molecules which are partially incorporated in the adjacent crystals. In the latter case the amorphous material can be considered as comprising of the molecules between adjacent crystals, loose ends (cilla), folds which protrude substantially from the fold surface and have collapsed, or of long traverses associated with a molecule which is incorporated into the same crystal at widely separated points (switchboard model) [5]. For a solution crystallized mat in which the crystals are formed as discrete entities prior to sedimentation, the molecules forming the amorphous layer must themselves belong to the geometrically defined single crystal [6, 7] (the second case considered above). It is therefore, hardly realistic to consider the structure of the fold surface and the nature of the amorphous layer as separate topics.

This last point is underlined by the selective degradation studies of Keller, Martuscelli, Priest and Udagawa [8]. They have shown that a certain proportion of the chain folds are buried within the crystal at various distances below its planar surfaces up to a maximum depth of 20 to 25 Å. They discuss various structural consequences of premature fold termination, pointing out that, on moving out through the crystal towards the fold surfaces, a critical concentration of such defects will be reached beyond which the lattice will either have to break up into relatively perfect crystal blocks with gaps between them, or spread evenly over the extra volume available and become equivalent to amorphous material. On the basis of the wide angle X-ray studies reported in this paper, the model of buried chain folds is both supported and developed.

1.2. Organization of this paper

Section 2 contains a review of the background diffraction theory on which the work is based. The theory of scattering for a one-dimensional paracrystalline lattice (due mainly to Hosemann and co-workers [10]) is developed for the case of an isolated diffraction peak with only low levels of distortion. In this form the theory is more readily applicable to the studies which follow.

Next (Section 3) calculations are made of the profile of the 002 diffraction peak and its correlation function for:

(a) various models of crystal shape profile in the [001] direction which reflect the distance over which the crystallinity is lost on moving out through the crystal towards the fold surfaces;

(b) various levels of paracrystalline lattice distortion in [001];

(c) possible Gaussian distributions of crystal thicknesses.

Particular attention is paid to the effect of these parameters on the intensities of the first subsidiary maxima of the diffraction peak, as these were experimentally observed (Fig. 8) and greatly add to the information which can be confidently extracted from the tails of the diffraction peak.

Section 4 is centred around the experimentally determined diffraction peak for the solution crystallized mat. Calculations based on the experimental quantitative determinations of the preferred orientation in the mats show that the 002 peak profile is not significantly modified by any overlapping peaks and that the observed subsidiaries do in fact belong to the 002 peak. Estimates are made of the influence of paracrystalline disorder and distribution of crystal thicknesses on the peak profile and a specific trapezium model proposed for the crystal shape function. The implications of this model are discussed in the context of previous work [8, 14, 15] and a specific proposal made concerning the structure of the fold surface.

2. Background theory

The diffracted intensity for a particular crystal direction (x) is given by the relation:

$$I_{(s)} = |F_{(s)}|^2 . \overbrace{\mathscr{F}[L_{\infty(x)}\,\phi_{(x)}]}^{2} \text{ per unit volume} \quad (1)$$

where $\mathscr{F}$ denotes Fourier transform and $\overbrace{\ }^{2}$ denotes the convolution of the product with itself.

$|F_{(s)}|$ is the structure factor of the crystal unit cell.

$L_{\infty(x)}$ is the lattice disposition function which may include distortion.

$\phi_{(x)}$ is the crystal shape function in the x direction.

In the case of an infinite crystal $\phi_{(x)} = 1$ and $\overbrace{\mathscr{F}[L_{\infty(x)}]}^{2}$ describes the reciprocal lattice which

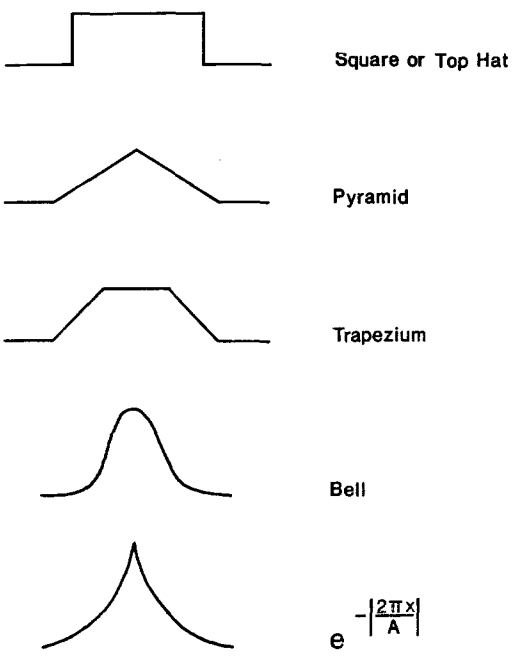

Figure 1 Various types of function referred to in the text.

will be modulated by the structure factor $|F|^2$ to give the diffracted intensity $I_{(s)}$.

For a crystal of finite size, limited by well defined surfaces perpendicular to the direction x, one can think in terms of a section of the infinite lattice disposition function "chopped out" by a square or "top-hat" function $\phi_{(x)}$. (See Fig. 1 for terminology used for various shapes of function.)

The reciprocal lattice points and hence diffraction peaks will be spread by a function which is the transform of the self convolution of $\phi_{(x)}$. So, in the absence of lattice distortion which also leads to peak broadening, the shape of a given diffraction peak due to scattering from (00l) crystal planes perpendicular to x will be determined directly by the crystal shape function:

$$\text{i.e. } I_{(s)00l} = |F_{(s)}|^2 . \overbrace{\mathscr{F}[\phi_{(x)}]}^{2} \text{ per unit volume} \quad (2)$$

Departures from the "top hat" shape functions can be a result of a decrease in crystal density near to the boundary surface due to lattice defects or surface re-entrants, or of surfaces which are not perpendicular to the x direction.

If crystals of limited size are stacked so as to produce a periodic density fluctuation in the x direction, the scattered intensity will be the product of $I_{(s)}$ of Equation 1 and the transform of the superlattice. In polymer systems the imperfection of the superlattice is generally sufficient to suppress sampling of all diffraction peaks except 000.

Paracrystalline distortions of the crystal lattice are described by the parameter $(\Delta_a/\bar{a})^2$ where Δ_a^2 is the mean square fluctuation in the average lattice period $\bar{a}$. It was first shown by Landau [9] that the self convolution of a lattice containing paracrystalline disorder can be represented by:

$$\overbrace{L_{\infty(x)}}^{2} = H_0 + \sum_{m=1}^{\infty} [\overbrace{H_1}^{m} + \overbrace{H_{-1}}^{m}] \quad (3)$$

where H_0 is a delta function and H_1 is the distribution function describing the statistical range of spacings between adjacent lattice points.

Hosemann and co-workers [10-12] have further developed this analysis and derived the scattering function $Z_{(s)}$ for a lattice with paracrystalline distortion:

$$Z_{(s)} = \overbrace{\mathscr{F}[L_{\infty(x)}]}^{2} = \sum_{m=1}^{\infty} [F_1{}^m + F_1{}^{*m}] + \mathscr{F}[H_0] \quad (4)$$

where F_1 is the transform of H_1 and $F_1{}^*$ its complex conjugate.

Now, $\mathscr{F}[H_0] = 1$ and the series

$$1 + \Sigma F_1{}^m = \frac{1}{1 - F_1}$$

and

$$1 + \Sigma F_1{}^{*m} = \frac{1}{1 - F_1{}^*}$$

therefore

$$Z_{(s)} = \left(\frac{1}{1 - F_1}\right) + \left(\frac{1}{1 - F_1{}^*}\right) - 1 \cdot \quad (5)$$

Writing $F_1 = |F|e^{2\pi s\bar{a}}$ and $F_1{}^* = |F|e^{-2\pi s\bar{a}}$

$$Z_{(s)} = \frac{1 - |F|^2}{1 + |F|^2 - 2|F|\cos 2\pi s\bar{a}} \cdot \quad (6)$$

If $(\Delta_a/\bar{a}) < (0.1/n)$, then the nth order reciprocal lattice point and hence diffraction peak will be effectively separate from its neighbours and span a limited range of s over which $|F|$ is effectively constant.

The 001 reciprocal lattice point will be centred at $s\bar{a} = 1$ and have a maximum amplitude:

$$Z_{\max^{(001)}} = \frac{1 - |F|^2}{1 + |F|^2 - 2|F|} = \frac{1 - |F|^2}{(1 - |F|)^2} \cdot$$

The normalized profile of 001 is then:

$$Z_{(s)}^{(001)} = \frac{1 - |F|^2}{1 + |F|^2 - 2|F|\cos 2\pi\tilde{a}s} \cdot \frac{(1 - |F|)^2}{1 - |F|^2}$$
$$= \frac{\frac{1}{2}|F|(1 - |F|)^2}{(1 + |F|^2)/2|F| - \cos 2\pi\tilde{a}s}$$
$$= \frac{\frac{1}{2}|F|(1 - |F|)^2}{(1 - |F|)^2/2|F| + 1 - \cos 2\pi\tilde{a}s} .$$

Because of the assumption that the reciprocal lattice point profile is narrow compared with the spacing of successive orders, the approximation:

$$1 - \cos 2\pi\tilde{a}s \approx \frac{(2\pi\tilde{a}s)^2}{2}$$

is valid. Therefore

$$Z_{(s)}^{(001)} = \frac{1}{1 + (2\pi\tilde{a}s)^2 \cdot (|F|/(1 - |F|)^2)} . \quad (7)$$

The profile of the 001 diffraction peak resulting from paracrystalline disorder is therefore Cauchy i.e. of the form

$$\frac{1}{1 + A^2s^2} .$$

The Fourier transform of such a peak (the correlation function) will be given by:

$$\overbrace{(L_{\infty(x)})^{001}}^{2} = \exp\left[-\left|\frac{x}{\tilde{a}}\left(\frac{1 - |F|}{|F|^{\frac{1}{2}}}\right)\right|\right] . \quad (8)$$

Now, Equation 1 can be rewritten as it applies to a distinct diffraction peak as:

$$I_{(s)}^{00l} = |F_{(s)}|^2 \cdot \mathscr{F}[\overbrace{(L_{\infty(x)})^{001}}^{2} \cdot \overbrace{\phi_{(x)}}^{2}] . \quad (9)$$

The peak shape for the case where both paracrystalline distortion and limited crystal size contribute to the broadening is therefore the transform of the product of the two functions:

(i) $\overbrace{(L_{\infty(x)})^{001}}^{2}$ which has the form $\exp(-|2\pi x/A|)$ where A is a measure of the disorder, and

(ii) $\overbrace{\phi_{(x)}}^{2}$ which is a pyramid function when $\phi_{(x)}$ is a square (top hat) profile, and gradually changes to a bell function as the crystal boundaries (as defined by $\phi_{(x)}$) become more diffuse.

In other words the profile of the observed peak is the convolution of two peaks; one representing the crystal shape function and the other the paracrystalline disorder of the lattice.

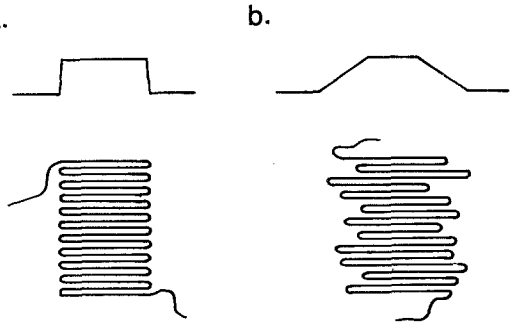

Figure 2 Model profiles for chain folded crystallites with (a) regular folding and (b) uneven folding which creates a diffuse fold surface.

A distribution of crystal sizes throughout the diffracting specimen leads to a straightforward superposition of the corresponding peak profiles and correlation functions.

For the case of a top hat crystal shape function and zero paracrystalline disorder, the second derivative of the correlation function gives the crystallite size distribution function [13]. So for (say) a Gaussian size distribution the correlation function appears qualitatively similar to that for paracrystalline disorder.

3. Relationship between the microstructure of polyethylene crystallites and the form of the 002 diffraction peak and its correlation function

3.1. A reasonable model for the crystal shape function in the chain direction [001]

The lamellar form of chain-folded polyethylene crystallites would suggest in the first instance a top-hat crystal shape function for the [001] direction, assuming of course, that the fold surfaces are parallel to the 002 planes. The destruction of the crystal lattice at the fold surface may well occur over transition region less than a few Angstroms thick (Fig. 2a) and the low angle measurements of Vonk [14] and Strobl and Müller [15] support this view.

It is possible, however, that the chain folding is not totally regular with the result that the folds are distributed above and below the mean position of the crystal surface. The profile in this case would have a trapezium form (Fig. 2b).

The realism of the trapezium model might be further improved by smoothing the sharp changes in curvature. In either case, however, the

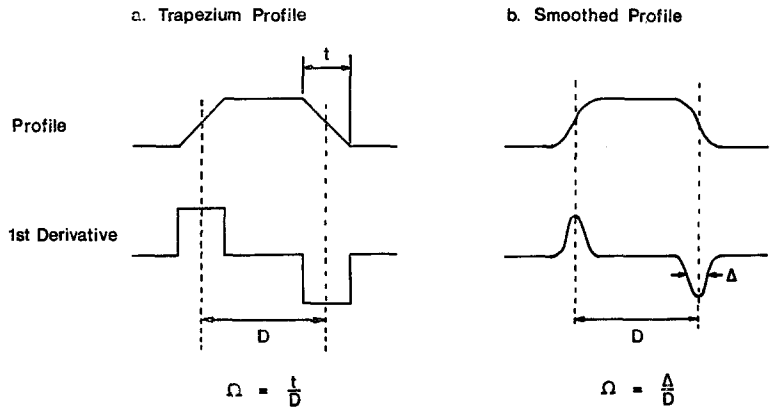

Figure 3 Two types of crystal profile with their first derivatives. The ratio of the width of the derivative peaks to their spacing is referred to as Ω and gives a measure of the thickness of the transition region at the fold surface.

thickness of the transition region is best described in terms of the first derivative of the crystal profile (Fig. 3). The parameter Ω is defined as the ratio of the half width of the peaks of the derivative function, to the distance between the peaks. So for the trapezium profile (Fig. 3a) $\Omega = t/D$ and for the smoothed profile (Fig. 3b) $\Omega = \Delta/D$.

The two extremes of the trapezium form, the square profile and the pyramid profile, correspond to values of $\Omega = 0.0$ and 1.0 respectively.

3.2. The effect of the profile function on the shape of the 002 diffraction peak

Equation 2 can be rewritten as:

$$I_{(s)}^{(00l)} = |F_{(s)}|^2 (\mathscr{F}[\phi_{(x)}])^2 .$$

Furthermore the transform of the first derivative. of $\phi_{(x)}$, $\mathscr{F}[\partial'(\phi_{(x)})]$, gives the first moment of the transform of $\phi_{(x)}$.

Now, the first derivative of the trapezium profile (Fig. 3a) can be described as the convolution of a square function and the transform of $\sin \pi s D$.

$$\text{i.e. } \partial'(\phi_{(x)}) = (\text{top hat}) \mathscr{F}[\sin \pi s D]$$

therefore

$$\mathscr{F}[\partial'(\phi_{(x)})] = \mathscr{F}(\text{top hat}) \,.\, \sin \pi s D = \frac{\sin \pi s t}{\pi s} \cdot \sin \pi s D$$

therefore

$$\mathscr{F}[\phi_{(x)}] = \frac{\sin \pi s t}{\pi s} \cdot \frac{\sin \pi s D}{\pi s}.$$

This function can be normalized by multiplying the terms by $1/t$ and $1/D$ respectively. Therefore

$$I_{(s)} = |F_{(s)}|^2 \left(\frac{\sin^2 \pi s t}{(\pi s t)^2} \cdot \frac{\sin^2 \pi s D}{(\pi s D)^2} \right). \quad (10)$$

The shape of the 002 diffraction peak for a crystal in which there is a transition region at the fold surface is the product of that corresponding to a crystal of the same average thickness but no transition region and another peak which is characteristic of the transition region. The latter peak is the square of the Fourier transform of the derivative of the crystal profile function in the transition region. Both peaks have the same maximum amplitude.

It is interesting to note that in the case of a trapezium profile with $t = D$ (i.e. $\Omega = 1$ making a pyramid function):

$$I_{(s)} = |F_{(s)}|^2 \left(\frac{\sin^4 \pi s D}{(\pi s D)^4} \right)$$

and the first subsidiary maximum of the function is reduced from 4.7% of the main peak amplitude (for the case of $\Omega = 0$) to 0.22%.

Equation 10 is essentially that given by Blundell [16] for the case of S.A.X.D. from crystals with trapezium density profiles. Its derivation in terms of the first derivative of the crystal profile however, respresents a new approach.

The analytical descriptions of the diffraction peak profiles for different values of Ω have been verified by numerically transforming self convolutions of the various crystal profiles.

The 002 peak profiles and the corresponding correlation functions for several values of x are given in Fig. 4a. The intensity of the first subsidiary maxima expressed as a proportion of the main peak intensity gives a ready measure

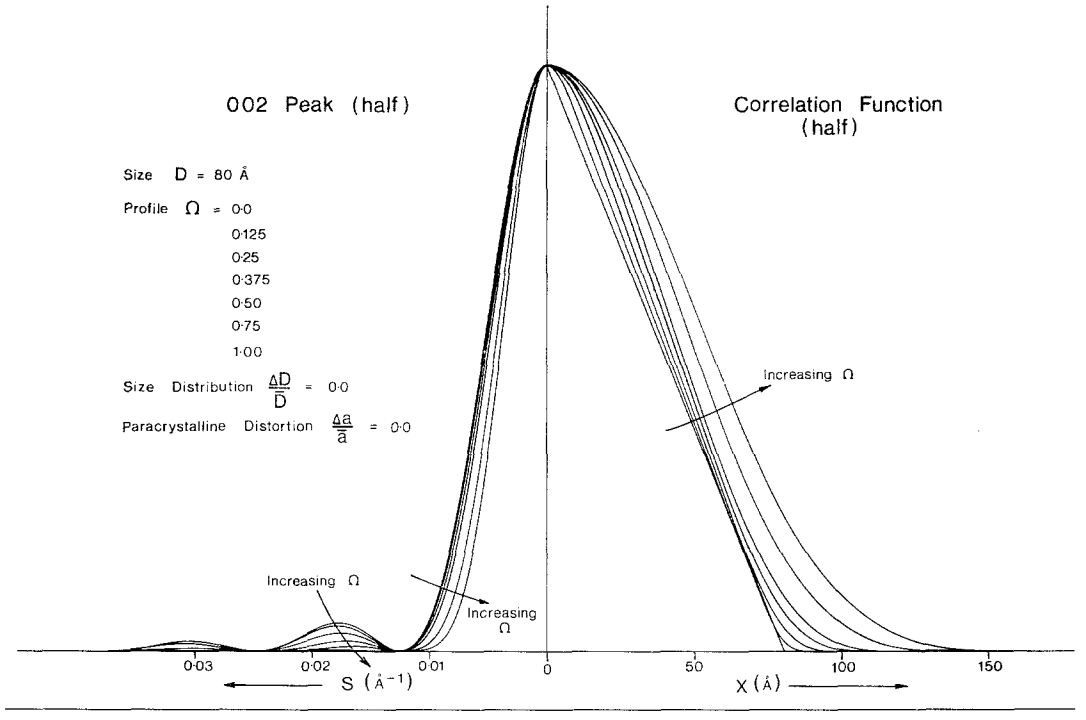
002 Peak (half)
Correlation Function (half)
Size D = 80 Å
Profile Ω = 0·0
0·125
0·25
0·375
0·50
0·75
1·00
Size Distribution ΔD/D = 0·0
Paracrystalline Distortion Δa/a = 0·0
Increasing Ω
Increasing Ω
Increasing Ω
0·03
0·02
0·01
0
50
100
150
S (Å⁻¹)
X (Å)

(a)

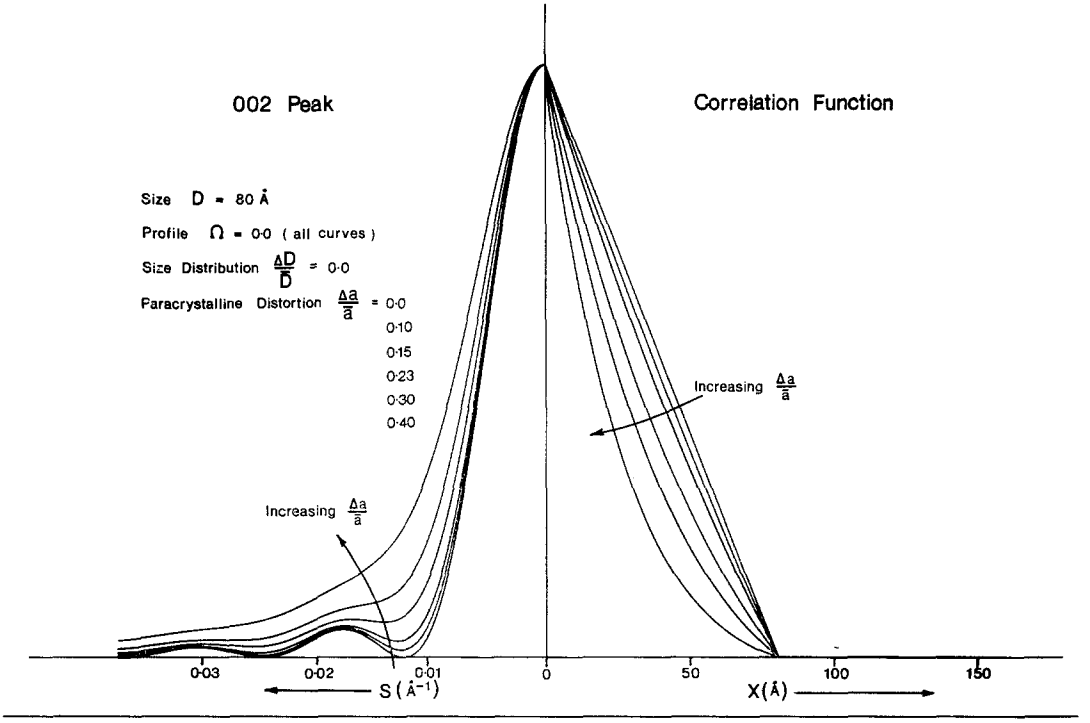
002 Peak
Correlation Function
Size D = 80 Å
Profile Ω = 0·0 (all curves)
Size Distribution ΔD/D = 0·0
Paracrystalline Distortion Δa/a = 0·0
0·10
0·15
0·23
0·30
0·40
Increasing Δa/a
Increasing Δa/a
0·03
0·02
0·01
0
50
100
150
S (Å⁻¹)
X(Å)

(b)

Figure 4

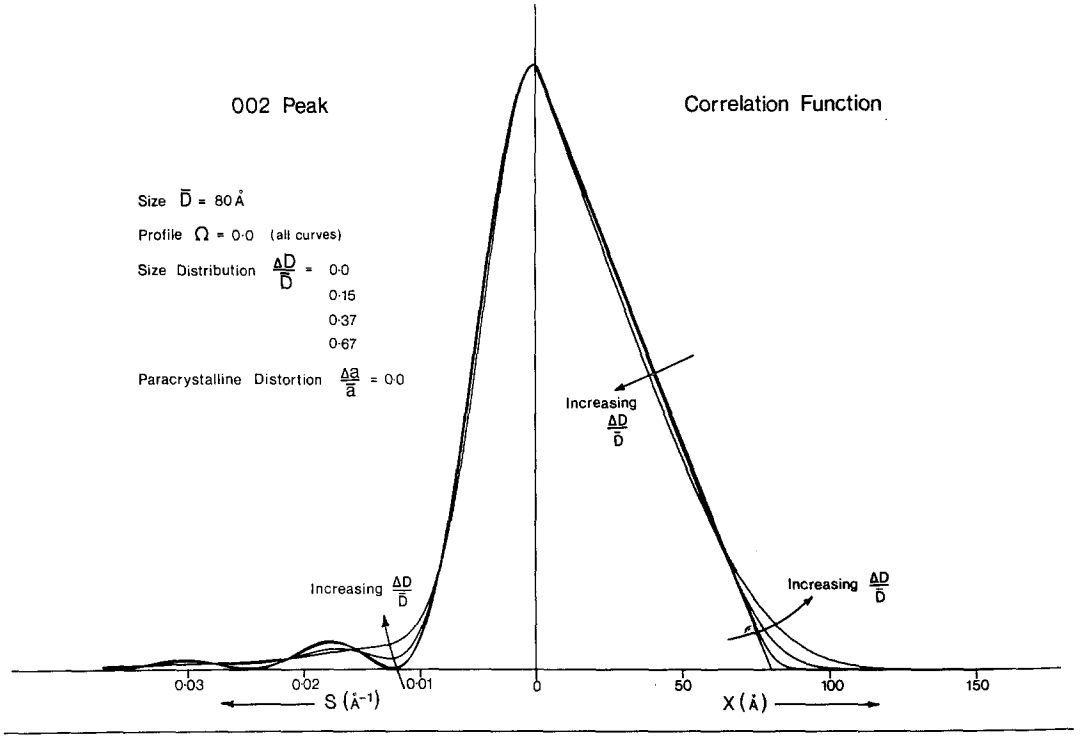

(c)

Figure 4 Calculated 002 peak profiles and correlation functions based on models which account for (a) a range of Ω values, (b) various levels of paracrystalline disorder and (c) Gaussian distributions of crystal sizes with different half widths.

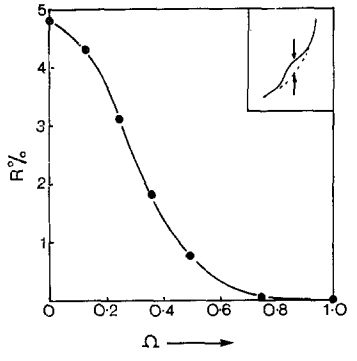

Figure 5 The dependence of R on Ω. R is defined as the ratio, expressed as a percentage, of the intensity of the first order subsidiary maxima to the main peak intensity. The background level for the subsidiary maxima is taken as the extrapolation of the curve of the main peak which is tangential to the tail of that peak beyond the subsidiary (see inset and Fig. 8 inset).

of the value of Ω. The relation between the subsidiary peak intensity and Ω is drawn in Fig. 5.

3.3. The influence of paracrystalline distortion of the 002 lattice planes on the diffraction peak

Equations 8 and 9 show that paracrystalline distortion can be taken into account by multiplying the correlation function by another function of the type $\exp(-|2\pi x/A|)$, where A depends on the degree of disorder. Accordingly this type of disorder has the effect of convoluting the diffraction peak (corresponding to a particular crystal shape function) with another peak of Cauchy form, the breadth of which increases with increasing disorder.

The effect of increasing degrees of paracrystalline disorder on the 002 diffraction peak and correlation function for a crystal of thickness 80 Å and $\Omega = 0$ is shown in Fig. 4b. The curves are calculated on the basis that the distribution function, H_1, is Gaussian in form. It can be seen that the convolution of the peak with the Cauchy function has the effect of smearing the subsidiary maxima as well as rounding the main peak. The maxima are not observable when

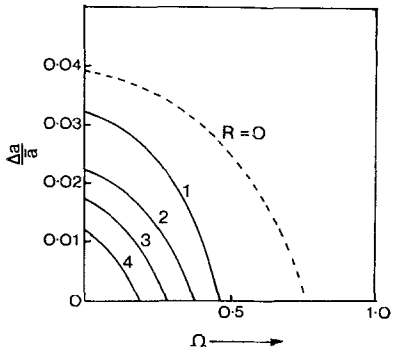

Figure 6 Contour map depicting R as a function of both Ω and the paracrystalline disorder Δ_a/a.

$\Delta_a/\bar{a}$ exceeds 0.03. the combined influence of increasing values of both Ω and $\Delta_a/\bar{a}$ on the subsidiary peak heights are summarized by Fig. 6.

3.4. The effect of a distribution of crystal sizes

It was first shown by Warren and Averbach [13] that for "top-hat" type shape functions the positive curvature of the correlation function is proportional to the number distribution function of the crystal size. The diffraction peaks and correlation functions shown in Fig. 4c are calculated for Gaussian shaped size distribution functions of varying widths, defined by $\Delta_D/\bar{D}$ where Δ_D is the half width of the Gaussian distribution and $\bar{D}$ the average thickness. For $\Omega = 0$ (top-hat shape function) the first subsidiary disappears when $\Delta_D/\bar{D}$ exceeds 0.55. Peak shapes have been calculated for various combinations of $\Delta_D/\bar{D}$ and Ω parameters, and Fig. 7 is prepared from this data.

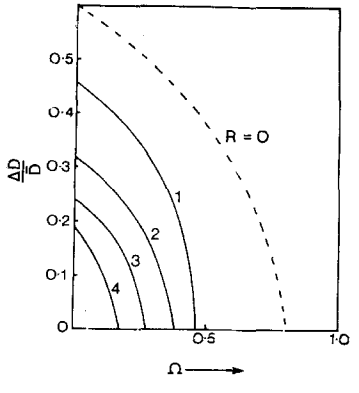

Figure 7 R as a function of $\Delta_D/\bar{D}$ (which is a measure of the range of crystal sizes present assuming a Gaussian distribution around $\bar{D}$) and Ω.

4. Measurement of the 002 diffraction peak of high density polyethylene

4.1. Specimens

High density polyethylene (RIGIDEX 50) was precipitated from 0.04% solution in xylene at 70°C and collected by filtering. Successive thin polymer mats were plied on top of each other prior to drying to produce a specimen 0.40 mm thick with well defined preferred orientation to enhance the 002 peak as recorded by reflection powder diffractometry. The ply technique was developed by Dr Y. Kobayashi [3], who prepared the stock material from which the specimens used in this work were cut.

Wide and low angle X-ray diffraction photographs of the mats confirmed that the polymer molecules were perpendicular to the lamellar crystallites which were, in turn, oriented predominantly parallel to the surface of the mat.

4.2. Scan of the 002 diffraction peak

Measurements of the profile of the 002 peak and of the scattered intensity over an angular range of 15° (2θ) centred on the peak, were made using a Philips horizontal diffractometer equipped with a step-scanning facility. The radiation used was nickel filtered CuK. The scan increments were 0.02° or 0.05° 2θ as appropriate and the statistical scatter of individual points brought within acceptable limits by counting for periods of 1000 secs.

Fig. 8 shows the results obtained. The 112 peak is as intense as 002 and close enough to cause some overlapping of the tails. Both peaks are superimposed on a diffuse halo which may be due to either diffraction from "amorphous" material or a reduction in the degree of longitudinal register of adjacent molecules in the crystal. The halo will only be considered here however, in as much as it complicates the estimation of the background level for the crystalline peaks.

On either side of the 002 peak are what appear to be first order subsidiary maxima with a suggestion of the second order on the low angle side.

4.3. Survey of the diffraction peaks in the region of 002 using an extended chain specimen of polyethylene

Before the shape of the 002 peak can be confidently analysed it is necessary to determine whether there are any overlapping peaks which are not obvious on account of their lower in-

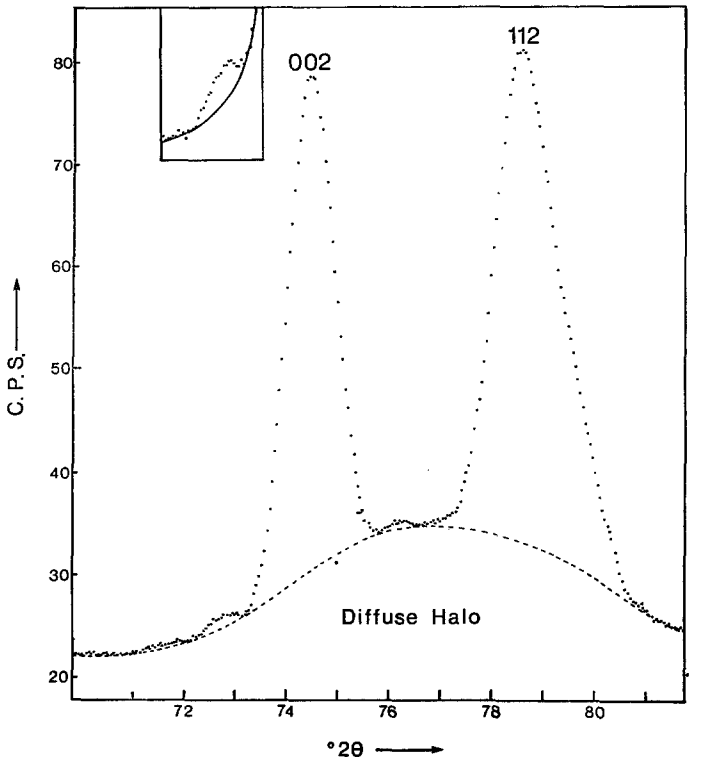

Figure 8 The 002 and 112 diffraction peaks of the solution crystallized mat showing the first order subsidiaries to 002. The count time per point was 1000 sec. The inset shows a scan of the lower angle subsidiary peak with a point count time of 4000 sec. (The c.p.s. scale for the inset is 4× that of the remainder of the figure.)

tensity and comparable breadth. In this context it is especially important to verify that the apparent subsidiary peaks to 002 are in fact genuine, as they will play a significant part in the analysis of crystallite microstructure.

The diffraction peaks of extended chain polyethylene are sharper than those of the normal material and accordingly a scan of such a specimen (Fig. 9) provides a useful basis for the identification of peaks close to 002 which may interfere with its analysis. The specimen used, which was supplied by Professor Wunderlich, had been crystallized under hydrostatic pressure so as to achieve complete or near complete chain extension [17].

The peaks 231, 421, 501 and 520 overlap 002, and 231 and the combination 421/501 are intense enough to be identified on Fig. 9. Whether they interfere with the measurement of the 002 peak profile of the solution crystallized specimen depends on the perfection of the texture of that specimen.

The texture was quantified by measuring the angular intensity distribution around the 110 and 200 rings recorded on film by transmission diffraction. Fig. 10 is a plot of intensity against the angle ϕ between the molecular axis and the perpendicular to the plane of the crystal mat. The intensity for both reflections is normalized to unity at $\phi = 0°$, the data having been obtained from three photographs of different exposure. Polyanyi's correction [18] was not deemed necessary in view of the low Bragg angle. The plot of $I \cos \phi$ versus ϕ on Fig. 10 gives the relative number of plane normals oriented at a given inclination ϕ for the angular range $\phi = 0$ to $\sim 75°$. On this basis the peaks 002, 231, 421, 501 and 520 are reduced in intensity on account of the texture by the factors given in Table 1.

The amount by which the intensity of the peaks in the angular region of 002 is reduced by thermal fluctuation depends strongly on the angle between the diffracting plane and the molecular axis of the crystal. This is because the molecules vibrate with particularly large amplitudes in directions perpendicular to their axes. The effect is strikingly shown in Fig. 11 which is a plot of the ratio of the peak intensity measured

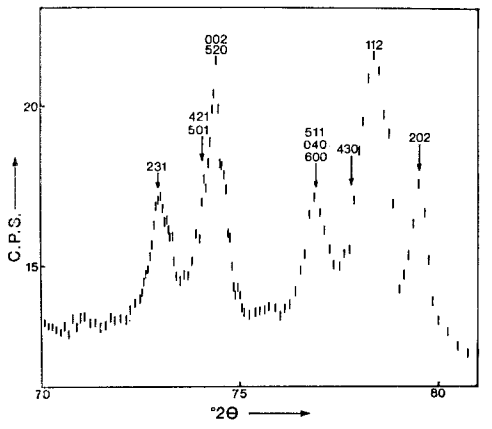

Figure 9 Scan of the peaks close to 002 from an extended chain specimen of H.D.P.E. The point count time was 400 sec and the vertical bars indicate the most probable statistical error for each point.

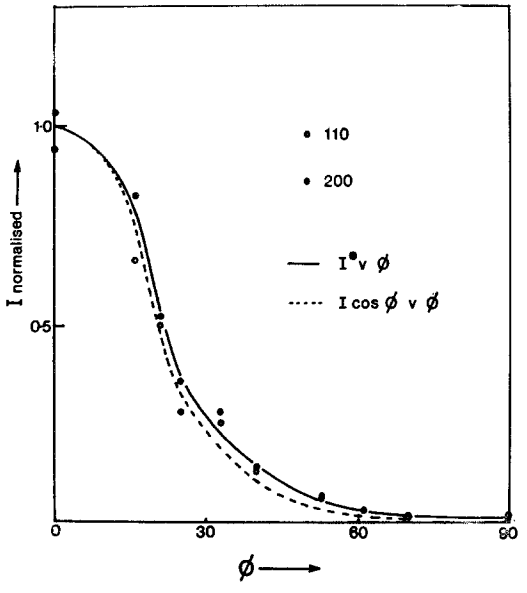

Figure 10 Plot of the intensity around one quadrant of the 110 and 200 diffraction rings obtained with the X-ray beam parallel to the plane of the mat. The data are normalized to unity at maximum intensity.

TABLE I

hkl	*hkl*^[001]	Reduction factor due to texture
002	0°	1.000
231	60°	0.015
421	60°	0.015
501	60°	0.015
520	90°	<0.01

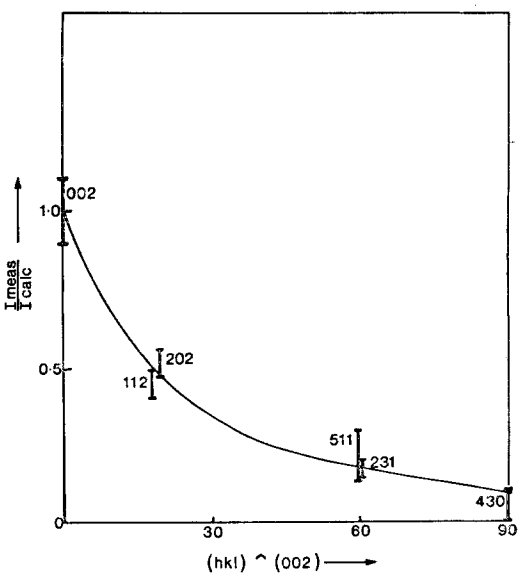

Figure 11 Plot of the ratio of peak intensity (measured from Fig. 9) to the calculated values *against* the angle between the diffracting planes (*hkl*) and the (002) plane. The ratio is normalized to unity for the 002 peak. The error limits for the 511 peak take into account the fact that the intensities of 040 and 600 which overlap it will be negligible.

from Fig. 9 to that calculated from the known crystal structure, against the angle between the plane normal and the 002 direction. The combination of the data in Table I with the measured ratios of peak heights from the unoriented (extended chain) specimen gives a measure of the relative intensity of the overlapping peaks for the oriented mat. These values are listed in Table II. In cases where peaks are not clearly identifiable in Fig. 9, their intensity has been gauged by interpolation of the data in Fig. 11.

These calculations indicate that with the possible exception of 231 none of the overlapping peaks will significantly affect the profile of 002. The calculated intensity of the 231 peak corresponds to about one third of the measured intensity of the subsidiary on the low angle side of 002. It appears, therefore, that the subsidiary is genuine but is reinforced by the presence of the 231 peak.

This conclusion is corroborated by the presence of another slightly less intense subsidiary on the high angle side of 002 in an angular region otherwise devoid of peaks.

Furthermore, annealing the crystal mat, which results in a narrowing of 002 due to the increase

TABLE II

hkl	$\frac{I_{hkl}}{I_{002}}$ (from Fig. 9)	$\frac{I_{hkl(calc)}}{I_{002(calc)}}$	$\frac{I_{hkl}}{I_{002}}$ (Calc. from interpolation of Fig. 11)	I_{hkl}/I_{002} (For textured mat)
002	1.00	—	—	1.00
231	0.45	—	—	0.006 75
421	—	0.84	0.18	0.002 70
501	—	0.43	0.09	0.001 35
520	—	0.97	0.11	< 0.001 1

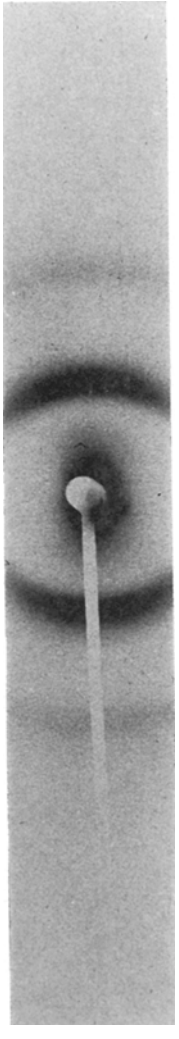

Figure 12 Low-angle photograph of the solution crystallized specimen.

in crystallite thickness, also leads to the disappearance of the subsidiaries (cf. Fig. 16). In view of the fact that there are no observable changes in texture on annealing, this is additional evidence that the 002 subsidiaries are genuine. There is, however, a small residual hump remaining at about 73° 2θ after annealing. This is most likely to be 231. The possible second order subsidiary at ~71.5° 2θ is not affected by annealing and its significance, if any, is not understood.

5. Analysis of 002 diffraction peak in terms of crystallite microstructure

5.1. Crystallite thickness

The positions of the well defined minima between the central peak and the subsidiaries are an excellent basis for the calculation of crystallite thickness (D). They are relatively insensitive to variations in the thickness of the transition layer at the fold surfaces, to paracrystalline distortion and also to size dispersion at levels which do not destroy the subsidiaries themselves. In addition the minima positions do not depend on a precise determination of the background level.

For the "as crystallized" mat the two minima are spaced at $\Delta s = 0.0242$ Å^{-1}.

$$\text{Now } D = \frac{2}{\Delta s}, \quad \text{therefore } D_{002} = 83.5 \text{ Å} \cdot$$

Small angle X-ray diffraction of the mat (Fig. 12) gave (using Bragg's equation) a long period of 111 Å.

5.2. Estimation of correct background level

The diffuse halo which spans the angular range 70° to 85° 2θ considerably complicates the determination of the correct background level. A smooth halo can be drawn in by eye, which corresponds to the measured intensity at points on each side of each subsidiary maximum (Fig. 8). In an attempt to check the validity of this estimate, the shapes of similar halos were measured for drawn melt crystallized samples of both low density and high density polyethylene. The average of these halos reduced to equivalent intensity, is plotted in Fig. 13 (curve B) where it can be compared with the estimate for the mat (curve A). The agreement in terms of profile is not particularly

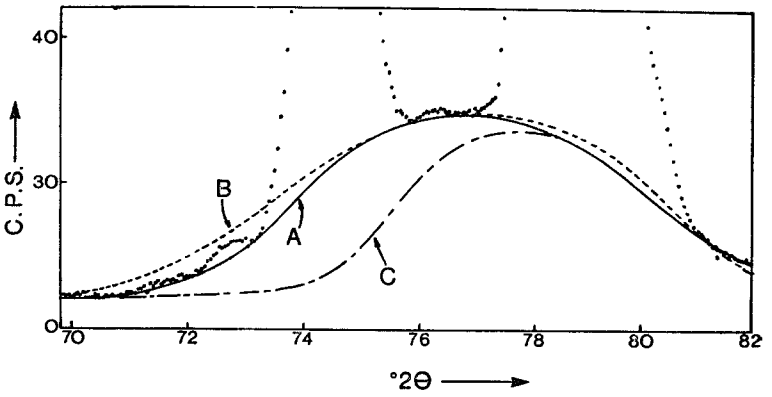

Figure 13 Three possible profiles for the diffuse halo: A, Best estimate possible by eye. B, Average profiles for similar halos measured from drawn samples of high and low density polyethylene. C, The required halo profile, if, the reduction in intensity of the subsidiary peaks from a maximum of 4.7% to the recorded 1.7% is due to paracrystalline distortion of the lattice alone and not a diffuse fold surface. (cf. Section 4.3 and Fig. 4b.)

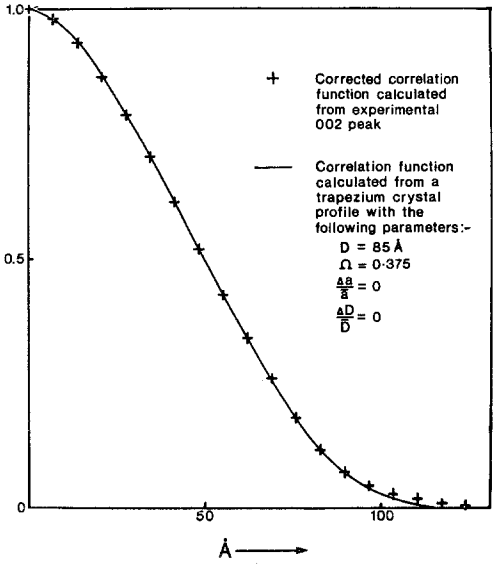

Figure 14 Experimental correlation function corrected for spectral, slit and absorption broadening compared with that calculated from the most appropriate crystal profile function ($\Omega = 0.375$, $D = 85$ Å).

good, but it seems to suggest that the actual intensity of the low angle part of the halo is unlikely to be less than that first estimated.

It is also significant that, although annealing reduced the width of the 002 peak and caused the disappearance of the subsidiaries, the halo profile is not noticeably changed (Fig. 16).

5.3. Determination of crystal profile

The crystal profiles have been estimated in three ways, although in each case a trapezium model was assumed.

(a) The subsidiaries of the measured 002 peak are 1.7% of peak intensity. On the basis of the estimate of background level made above, which is tantamount to assuming that there is zero paracrystalline disorder and no dispersion of crystallite thickness, the Ω parameter as read from Fig. 5 is 0.375.

(b) A curve matching routine was applied between the correlation function of the recorded peak which had been corrected for spectral and slit width and absorption broadening using Stokes' method [19], and the computed functions of the model profiles (Fig. 14). The best fit was obtained for $\Omega = 0.375$ and $D = 85.0$ Å.

(c) A direct measure of the thickness of the transition layer (t) can be obtained by using the method applied by Vonk [14] to low angle scattering.

The equation used is:

$$t = 2\left(\frac{d\gamma}{dx}\right)_{x=t} \Big/ \left(\frac{d^2\gamma}{dx^2}\right)_{x=0} \qquad (11)$$

and is applied to the corrected correlation function (γ plotted against x). The value obtained is 28 Å which corresponds to $\Omega = 0.34$ for $D = 85.0$ Å.

The agreement between the values for D and Ω (83.5 Å, 0.375) obtained from observation of the angular spacing of the first minima and the intensity of the first subsidiaries in relation to that of the main peak on the one hand, and the corresponding values (85.0 Å, 0.375) obtained by fitting model correlation functions to the corrected experimental functions on the other, reflects the fact that the breadth of the 002 peak is large compared with the additional slit,

spectral and absorption broadening due to the experimental method. The value for Ω (0.34) obtained by direct analysis of the corrected correlation function (Vonk's method) is encouragingly close to that obtained by the other two methods.

The values obtained by method (b) will be taken as definitive for the purposes of this paper, i.e. $D = 85.0$ Å, $\Omega = 0.375$.

The estimates for Ω are sensitive to the particular background level chosen. If the true background is in fact lower than that assumed above giving a corrected intensity at the first minima of greater than zero, then the transition region at the fold surface will be thinner than that corresponding to $\Omega = 0.375$, and paracrystalline distortion and/or dispersion of crystallite sizes will have made a contribution to reducing the subsidiary maxima height to the values recorded.

An upper limit for the size dispersion can be estimated from the low angle photograph (Fig. 12). The existence of at least two if not three "prominent" orders means that the paracrystalline disorder of the superlattice cannot exceed $\Delta_D/\bar{D} \approx 0.09$ [20]. If it is assumed that any variation in crystal thickness manifests itself as disorder of the superlattice (and is not exactly compensated by complimentary fluctuations in the intercrystallite layer thickness, nor simply a gradual variation across the bulk sample), it follows that the crystal size dispersion is less than ~0.09 and will not significantly affect the measured value of Ω (cf. Fig. 7).

It is not so easy to obtain an independent measure of the paracrystalline distortion of the crystal lattice, and we must rely more heavily on the accuracy of the estimate of background level. However, it is reassuring that Hosemann and co-workers [11, 12], who have made a three-dimensional survey of paracrystalline disorder in polyethylene, put a zero value on this parameter in the chain direction. Also Schönfeld and Wilke's [21] measurements of 002 width on extended chain specimens indicate for the chain direction a crystal size in excess of 5000 Å and negligible paracrystalline disorder. Their result is also confirmed by the data plotted in Fig. 15 which shows that the shape of the 002 peak of the extended chain specimen corresponds closely to that of the silicon 331 peak used as a standard after it has been corrected to take into account the broadening due to absorption (or rather lack of absorption) in the polyethylene specimen.

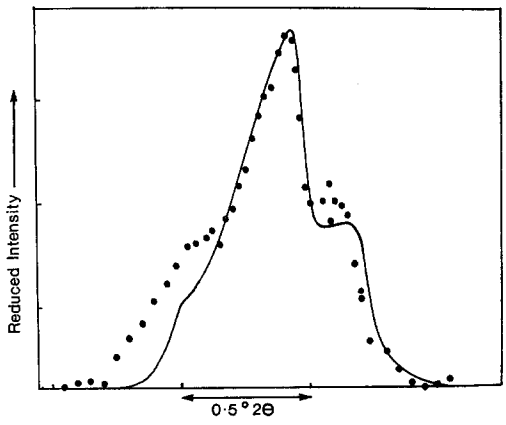

Figure 15 Comparison between the recorded 002 peak from the extended chain specimen (separate points) and the standard peak (continuous) which accounts for spectral, slit and absorption broadening. The knee on the low angle side of the standard peak is introduced when the absorption correction is made for the polyethylene specimen of finite thickness (0.94 mm). It would be absent if the specimen was very thick. The relatively poor agreement at lower angles is the result of the superimposition of the 421 and 501 peaks at ~73.9° 2θ.

In addition, if the thickness of the transition layer at the fold surface is zero and R, the ratio of subsidiary to main peak intensity, reduced to 1.7% by paracrystalline disorder alone, then the first minima will be at 7% and the second minima at 3% of the main peak height. To account for such a peak the diffuse halo forming the background would have to be substantially modified as in Fig. 13 (curve C). This amounts to assuming that the halo profiles measured from various bulk samples (as summarized in curve B) are considerably in error, the low angle side of the halo really belonging to the 002 peak. The fact that this is not the case and that profile (C) is indeed unrealistic is confirmed by X-ray scans of drawn bulk polyethylene, oriented so as to completely suppress 002, which show a halo profile equivalent to curve B not C.

6. Statement of proposed model and discussion

It has been argued that both dispersion of crystal sizes and paracrystalline disorder in the [001] direction are negligible for the solution crystallized mats examined. On this basis the predicted crystal profile is that drawn in Fig. 17.

The error limits are estimates only. The particularly large negative limit (~30%) put on the thickness of the transition layer at the fold

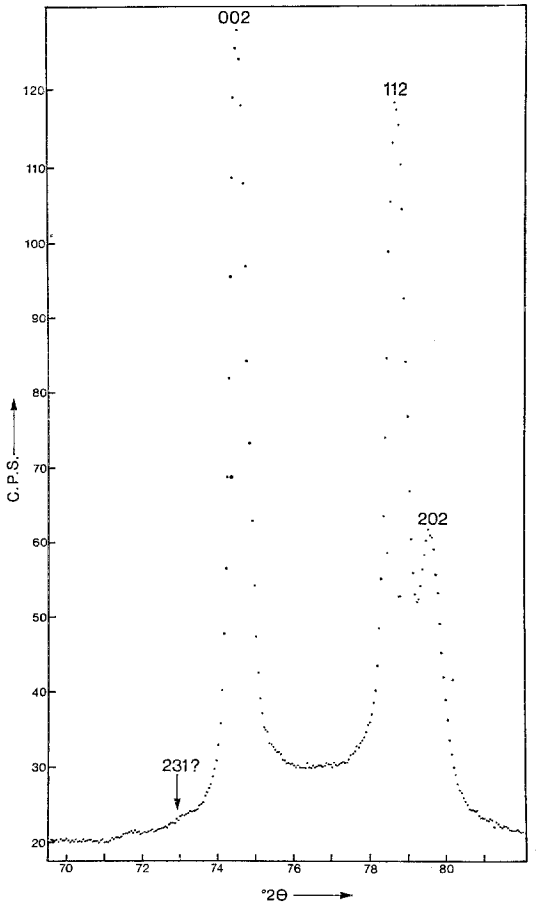

Figure 16 The 002, 112 and 202 diffraction peaks of a solution crystallized mat which has been annealed for 1.1×10^3 sec at 125°C. The count time per point was 1000 sec.

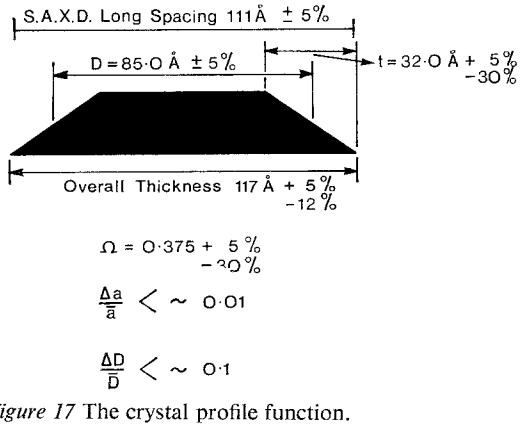

Figure 17 The crystal profile function.

surface takes into account the maximum levels of paracrystalline disorder and crystal size dispersion which could be present.

The fact that the overall crystal thickness ($D + t$ for this model) is, within experimental error, the same as the S.A.X.D. long period must in itself cast some doubt on the strict relevance of the two phase model to solution crystallized and sedimented mats.

The reduction in microcrystallinity on moving out through the transition zone between crystalline and amorphous regions can be interpreted in terms of the uneven fold length model (Fig. 2b), however such a model would imply a density defect of ~25% whereas 2.5% is typical of mats prepared by solution crystallization [22]. The model is also, at first sight, in conflict with the low angle measurements of Strobl and Müller on similar specimens [15], which indicate a transition zone of the order of 5 Å thick (equivalent to $\Omega = 0.059$ for our crystals).

The model (Fig. 17), however, need not represent density defects alone. Strictly it represents the fraction of atoms which are based on crystal lattice sites. It is probable therefore that there is an increasing level of disorder as the fold surfaces are approached. There must of course, be a density deficiency associated with any significant level of disorder, but this would be less than that envisaged in the buried fold model drawn in Fig. 2b, and need not conflict with the experimental density measurements.

A question now arises as to the interpetation of the disordered regions in terms of X-ray diffraction. Does the disorder contribute to the average level of paracrystallinity in the crystal and imprint the 002 peak accordingly; or is it best considered as a distinct amorphous phase, which will make its contribution to diffraction as a diffuse halo?

The latter model appears to be in better accord with the experimental evidence, i.e. the very low level of paracrystallinity in [001], and the observation of diffuse halos which may well represent diffraction from the amorphous component of the crystal. The implication being that there are crystalline and amorphous regions within the crystal entity but (for [001]) no gradual transition involving increasing levels of paracrystallinity between the two states.

The apparent gradual decrease in the crystalline/amorphous ratio over some 30 Å, as indicated by the trapezium crystal profile of Fig. 17, is most readily reconciled with a discontinuous transition between crystalline and amorphous material, by assuming that there is an increasing frequency of amorphous regions as

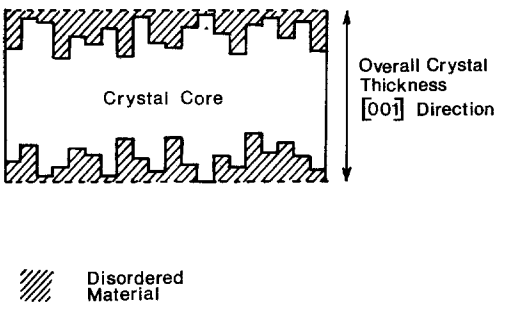

Figure 18 A schematic diagram showing the distribution of amorphous and crystalline regions which would account for the wide-angle X-ray (and density) observations.

the fold surface is approached. Such an arrangement is envisaged in Fig. 18.

The concept of buried folds developed by Keller, Martuscelli, Priest and Udagawa [8] offers an explanation in molecular terms of the distribution of amorphous regions outlined above. These authors proposed several specific structural elements involving buried or protruding folds. For a deeply buried fold they suggested the structure reproduced in Fig. 19a in which the perfect lattice is reformed at some distance above a buried fold. However, on account of the plane of symmetry at the centre of the crystal, the stresses associated with the buried folds will not be able to be relaxed by bending, and there will develop above each buried fold a region of hydrostatic tension extending up towards the fold surface. One result of this stress state is that the crystal melting point will be lowered. Extrapolation of the data of Matsuoka [23] for the pressure range +1 bar to +1 kbar predicts a reduction in melting point of 70°C per kbar of hydrostatic tension [24]. The bulk modulus of polyethylene is of the order of 50 kbar [25] which strongly suggests that the polymer chains in the region immediately above a buried fold will be above the local melting point at room temperature. It will be unreasonable to expect the chains in the localized molten regions to be completely random. Rather they will tend to assume a nematic liquid crystal type configuration, that is, lacking long range order but still possessing considerable longitudinal alignment. These nematic zones, already broadly envisaged by Keller *et al.* [8], are sketched schematically in Fig. 19b. It is interesting to note that beneath the buried fold there will be a region within which the crystal melting point is locally raised.

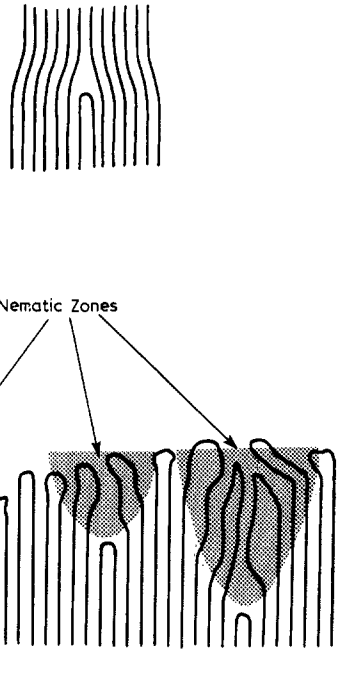

Figure 19 (a) Crystal defect due to a single fold buried deep inside the crystal [8]. (b) Buried folds accompanied by zones of nematic material.

A gradually increasing density of nematic zones as the fold surface is approached will account for the structural conclusions already drawn from the analysis of the 002 peak. Namely:

(i) A decrease in the amount of fully crystalline material as the fold surfaces are approached. Also, a small overall density defect which indicates that the crystalline material must be replaced by non-crystalline disordered material rather than just voids.

(ii) The very low level of paracrystallinity within the crystal for the [001] direction which indicates that the loss of order is discontinuous, and that the level of disorder is uniformly high, approaching that of amorphous material.

In an attempt to reconcile these results with those of Strobl and Müller [15], it can be suggested that a gradual decrease in density as the fold surfaces are approached (such as might be associated with an increased concentration of nematic zones) may well be dominated, as far as S.A.X.D. is concerned, by a more localized decrease in density within the highly disordered regions at the plane of contact of adjacent crystallites. Such a density variation within the

amorphous material would not influence the profile of the 002 peak.

The low angle measurements reported by Vonk [14] which broadly agree with those of Strobl and Müller, were made on melt crystallized material and for this reason are not strictly comparable with those discussed here.

The analysis presented in this paper does not take into account the influence of non-zero orders of temperature diffuse scattering on the profile of the 002 peak [26, 27]. The zero order scattering itself has no effect on the peak profile and is only of significance when considering the relative intensity of peaks adjacent to 002 (Fig. 11).

The treatment of paracrystalline distortion used in this study applies strictly to the case where the distortion distribution function, H_1, does not vary in any systematic way across the thickness of the crystal. On this basis, no [001] paracrystalline disorder was detected by experiment. It is, however, conceivable that the change in character of the immediate environment of a chain as it nears the fold surface (due perhaps to an adjacent nematic zone), coupled with the increasing proximity of the fold itself, will give rise to a slight, but progressive decrease in the spacing of the 002 planes. In this case the crystal profile would have both real and imaginary parts, and it is possible that the interpretation of the 002 peak profile may have to be modified to account for this new factor.

The consideration of non-zero order thermal diffuse scattering and the projection of the crystal profile function into the complex domain represent additional refinements of the analysis so far presented. Together they will form the subject of further work.

7. Conclusions

(a) The profile of a diffraction peak from an infinite crystal with some degree of paracrystalline disorder is Cauchy, i.e. of the form $1/(1 + A^2s^2)$, and the corresponding correlation function has the form $\exp(-|2\pi x/A|)$.

(b) The profile of a diffraction peak when both paracrystalline disorder and limited crystal size contribute to broadening is the convolution of two peaks which would correspond to the separate contributions of disorder and limited size.

(c) When a crystal shape function of trapezium form (for [001]) is defined in terms of the spacing (D) and width (t) of the two peaks forming its derivative, the shape of the corresponding diffraction peak is given by

$$I_{(s)00l} \propto \left(\frac{\sin^2\pi st}{(\pi st)^2} \cdot \frac{\sin^2\pi sD}{(\pi sD)^2}\right) .$$

(d) Analysis of the 002 diffraction peak of solution crystallized polyethylene shows that:

(i) The overall crystalline thickness (117 Å) is of the same order as the long period measured by S.A.X.D. (111 Å).

(ii) There is a reduction in the percentage of atoms based on lattice sites (microcrystallinity) on moving out from the centre of the crystallites to the fold surfaces. In terms of the trapezium model of the crystal profile the microcrystallinity decreases from 100% to zero over a distance of 32 Å.

(iii) The level of paracrystalline distortion in [001] was too low to be apparent in the analysis of the 002 peak.

(iv) S.A.X.D. indicates a low level of paracrystalline disorder in the superlattice. On this basis the predicted statistical variations in the thickness of the lamellae will not be sufficient to be detected by the analysis of the 002 profile. The observed profile bore no evidence of any significant dispersion of crystal thickness.

(e) The reduction of microcrystallinity in the region of the fold surfaces cannot be accounted for solely in terms of an increasing density of voids above buried folds, for the overall density defect would far exceed that measured. The low level of microcrystallinity near to the fold surfaces must correspond to a high level of disorder.

(f) The 002 peak profile gives no indication of any paracrystalline disorder in [001], although it is superimposed on a diffuse halo which suggests that some material is present in the specimen with a level of disorder which approaches that typical of amorphous material.

(g) The observations outlined in (e) and (f) can be reconciled in terms of the buried fold model [8]. It is proposed that the hydrostatic tension above a buried fold lowers the melting point within a localized zone to below room temperature. The structure within such a zone however will be more similar to that of a nematic liquid crystal than to the random coil arrangement typical of the fully amorphous material.

Acknowledgements

This work was started at the instigation of Professor Keller and has continued with his constant encouragement and guidance. Much of

the experimental work was carried out during a period spent at the H. H. Wills Physics Laboratory at Bristol University. The author is also indebted to Dr Y. Kobayashi for his preparation of the solution grown mats, to Professor B. Wunderlich who supplied the extended claim specimen, and to Professor F. C. Frank, Dr E. Atkins, Dr M. Folkes, Dr D. Sadler and Dr A. Schönfeld for stimulating discussions and helpful suggestions. The low-angle photograph (Fig. 12) was taken by Dr Folkes.

References

1. A. KELLER, *Phil. Mag.* **8** (1957) 1171.
2. W. O. STATTON in "Newer Methods of Polymer Characterisation", (edited by B. Ke) (Interscience, New York, 1964) Chapter 6.
3. Y. KOBAYASHI and A. KELLER, *J. Mater. Sci.* **9** (1974) 2056.
4. H. G. THIELKE and F. W. BILLMEYER, *J. Polymer Sci. A.* **2** (1964) 2947.
5. P. J. FLORY, *J. Amer. Chem. Soc.* **84** (1962) 2857.
6. A. KELLER, *Rep. Progr. Phys.* **31** (1968) 623.
7. A. KELLER, *Kolloid-Z.Z. Polym.* **231** (1969) 386.
8. A. KELLER, E. MARTIUSCELLI, D. J. PRIEST and Y. UDAGAWA, *J. Polymer Sci. A2*, **9** (1971) 1807.
9. L. D. LANDAU, *Zhurnal Eskperimentalnoi I Teoreticheskoi Fiziki*, **7** (1937) 1227.
10. R. HOSEMANN and S. N. BAGCHI, "Direct Analysis of Diffraction by Matter", (North Holland, Amsterdam, 1962).
11. W. WILKE, W. VOGEL and R. HOSEMANN, *Kolloid-Z.Z. Polym.* **237** (1970) 317.
12. A. SCHÖNFELD, W. WILKE, G. HÖHNE and R. HOSEMANN, *ibid.* **250** (1970) 102.
13. B. E. WARREN and B. L. AVERBACH, *J. Appl. Phys.* **21** (1950) 595.
14. C. G. VONK, *J. Appl. Cryst.* **6** (1973) 81.
15. G. R. STROBL and N. MÜLLER, *J. Polymer Sci. A2* **11** (1973) 1219.
16. D. J. BLUNDELL, *Acta. Cryst.* **A26** (1970) 476.
17. B. WUNDERLICH *et al.* A series of papers: *J. Polymer Sci. A*-2 **7** (1969) from 2043.
18. M. POLANYI, *Z. Physik.* **7** (1921) 149.
19. A. R. STOKES, *Proc. Phys. Soc. Lond.* **61** (1948) 382.
20. R. HOSEMANN, *Acta Cryst.* **4** (1951) 520.
21. A. SCHONFELD and W. WILKE, *Kolloid-Z.Z. Polym.* **250** (1972) 496.
22. D. A. BLACKADDER and P. A. LEWELL, *Polymer* **9** (1968) 249.
23. S. MATSUOKU, *J. Polymer Sci.* **57** (1962) 569.
24. A. PETERLIN, *J. Mater. Sci.* **6** (1971) 490.
25. A. ODAJIMA and T. MAEDA, *J. Polymer Sci. C* **16** (1966) 55.
26. B. E. WARREN, "X-ray Diffraction", (Addison-Wesley, London, 1969) p. 162.
27. W. A. KELLER, *Acta Cryst.* **A28** (1972) 328.

Received 25 June and accepted 27 August 1974.